ELSEVIER

Journal of Alloys and Compounds 446–447 (2007) 332–335

Journal of ALLOYS AND COMPOUNDS

www.elsevier.com/locate/jallcom

Reaction steps in the Li–Mg–N–H hydrogen storage system

W. Lohstroh*, M. Fichtner

Institut für Nanotechnologie, Forschungszentrum Karlsruhe, Postfach 3640, 76021 Karlsruhe, Germany

Received 27 September 2006; received in revised form 7 December 2006; accepted 18 December 2006
Available online 21 December 2006

Abstract

The reaction steps in mixtures of $2LiNH_2$–MgH_2 during hydrogen sorption are investigated. Differential scanning calorimetry experiments at various H_2 pressures show that the initial decomposition comprises several steps and their transition temperature depends on the applied hydrogen pressure. During the first desorption of the powders, an exothermic phase transition takes place where $Mg(NH_2)_2$ is partially formed. This is followed by an endothermic decomposition that yields hydrogen. The addition of 2 mol% $TiCl_3$ to the initial $2LiNH_2$–MgH_2 mixture does not affect the exothermic phase transition but the hydrogen release shifts to lower temperatures. Adding 2 mol% $TiCl_3$ after two hydrogenation cycles to the material has no effect on the desorption properties.

Keywords: Hydrogen storage; Complex hydride; $LiNH_2$; $Mg(NH_2)_2$

1. Introduction

In view of a future hydrogen economy, safe and reliant storage facilities for hydrogen have to be developed. For automotive applications the capacity of the storage system should exceed >5 wt.% hydrogen in the system and ideally the desorption temperature is adjusted to the working temperature of membrane fuel cells. Among the promising candidates for solid storage materials that have potential to fulfil these conditions are reactive hydride composites combining complex hydrides (e.g. $LiBH_4$ [1] or $LiNH_2$ [2]) with binary hydrides such as LiH. Chen et al. [2] proposed the system $LiNH_2 + LiH$ which can store theoretically up to 10.5 wt.% H_2. For practical applications only the first decomposition step can be used (6.5 wt.% H_2) as the required temperatures for the second step (above 300 °C) are too high. Substitution of LiH by MgH_2 lowers the decomposition temperature while the storage capacity (of the first step) decreases to 5.6 wt.% [3].

For the Li–Mg–N–H system it was found that it can deliver 30 bar H_2 at 200 °C [4,5]. The proposed reactions can be described by

$$2LiNH_2 + MgH_2 \rightarrow Li_2NH + MgNH + 2H_2 \quad (1)$$

$$Mg(NH_2)_2 + 2LiH \leftrightarrow Li_2NH + MgNH + 2H_2 \quad (2)$$

where reaction (1) takes place during the first desorption while subsequent sorption cycles follow reaction (2). For the products of both reactions a mixed phase of the composition $Li_2Mg(NH)_2$ has also been proposed [4]. It has been suggested that it could be formed in to a solid state reaction between the two imide phases MgNH and Li_2NH [6]. However, this phase is still under discussion and its structure has to be further elucidated. Desorption at $T \geq 400$ °C results in further decomposition with Mg_3N_2 and Li_3N as final products [6]. In this paper, we will report on the reaction steps that take place during the first and subsequent sorption cycles.

2. Experimental

Mixtures of $LiNH_2$ and MgH_2 have been prepared by ball milling in a planetary ball mill (ball to powder ratio 20:1, 600 rpm, Si_3N_4 vial). For the caloric measurements a Netzsch high pressure differential scanning calorimeter (DSC) HP-DSC 204 was used at various hydrogen pressures. For structural characterization X-ray diffraction (Cu Kα = 0.15418 nm) and IR-spectrometry were used. Additionally, the hydrogen and ammonia release (which is emitted as an unwanted by-product) was monitored in a Netzsch STA409 TG–MS system under high vacuum conditions. All handling of the powders was done in inert atmosphere in an argon filled glove box with partial pressures of oxygen and water below 0.1 ppm. Hydrogen desorption/absorption cycles are performed in a modified Sievert's apparatus, for a detailed description

* Corresponding author.
E-mail address: wiebke.lohstroh@int.fzk.de (W. Lohstroh).

0925-8388/$ – see front matter © 2007 Elsevier B.V. All rights reserved.
doi:10.1016/j.jallcom.2006.12.060

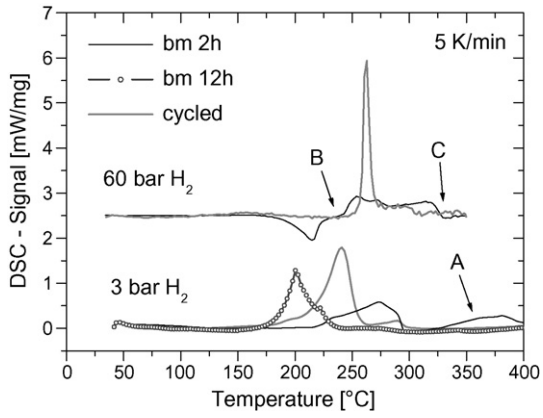

Fig. 1. DSC measurements for $2LiNH_2$–MgH_2: (a) 3 bar H_2 and ball milled 2 h (black line), 12 h (open circles) and after two desorption/absorption cycles (gray line) (b) at 60 bar H_2: after 2 h ball milling, and after two absorption desorption cycles. For clarity, the curves have been shifted along the *y*-axis. The labels A–C refer to points at which FTIR experiments were performed.

of the apparatus see Ref. [7]. The conditions for desorption were $T_{des} = 230\,^{\circ}C$, 0.3 bar H_2 and for absorption $T_{abs} = 200\,^{\circ}C$, 100 bar H_2.

3. Results

3.1. Undoped system

Fig. 1(a) shows DSC data at 3 bar H_2 of $2LiNH_2$–MgH_2 mixtures ball milled for 2 h and after two hydrogen sorption cycles have been completed. Additionally, the DSC-signal of a sample ball milled for 12 h has been included. After milling 2 h (solid line), we observe a small exothermic reaction around 215 °C where $Mg(NH_2)_2$ is formed at least partially (see below). This is followed by a broad endothermic peak around 260 °C corresponding to hydrogen release. The two subsequent steps are better resolved at 60 bar H_2 pressure (see Fig. 1(b)) where the exothermic transition is clearly separated from the ensuing decomposition reaction. Prolonged milling of the initial mixture for 12 h supplies the necessary energy for the exothermic transition to form $Mg(NH_2)_2$ directly during milling. Furthermore, the hydrogen release is shifted to lower temperatures: the DSC signal only exhibits an endothermic transition around 200 °C. This is in agreement with earlier results [8] that have been reported for the $Mg(NH_2)_2$–2LiH system [9].

After cycling the material, only one endothermic peak appears. The sample initially ball milled 2 h, decomposes around 240 °C while T_{des} remains unchanged (around 200 °C) for the sample initially ball milled 12 h (not shown).

Fig. 2 displays IR spectra at various stages of the reaction. The characteristic IR absorptions are located at 3325 and 3274 cm^{-1} for $Mg(NH_2)_2$ [4,10], and at 3313 and 3259 cm^{-1} for $LiNH_2$ [11], respectively. In the desorbed state, MgNH shows a strong absorption line at 3197 cm^{-1} [10] and Li_2NH at 3162 cm^{-1} [11]. After 2 h milling, $LiNH_2$ is identified in the IR spectra. In contrast, after 12 h milling time the sharp $LiNH_2$ lines disappeared and a broad absorption around 3267 cm^{-1} is observed indicating at least partial formation of $Mg(NH_2)_2$. This is supported by

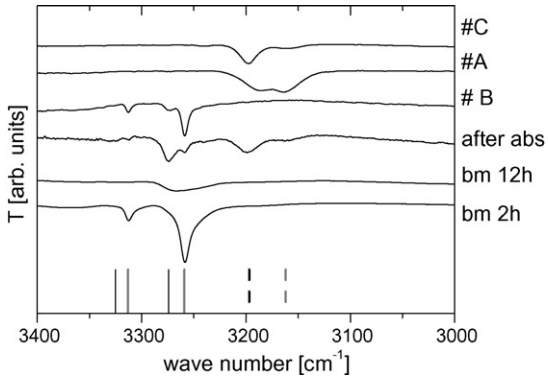

Fig. 2. IR spectometry after 2 h milling, 12 h milling, and after two sorption cycles. #A–#C are measured after DSC experiments as indicated in Fig. 1. The solid lines mark the characteristic absorption frequencies for $LiNH_2$ and $Mg(NH_2)_2$ and the dashed markers indicate the location of the imide absorptions.

X-ray diffraction data which show crystalline $LiNH_2$ and MgH_2 after 2 h milling time (see Fig. 3) while after 12 h milling time only scarce diffraction peaks are observed and the main part of the sample is X-ray amorphous. After two sorption cycles, $Mg(NH_2)_2$ is clearly visible in IR and XRD data, furthermore $LiNH_2$ appears. Apparently, the reabsorption has been incomplete as indicated by the MgNH IR-lines around 3197 cm^{-1}. This can explain the capacity during cycling which amounts to ≈ 3.5–4 wt.% only in comparison to the theoretical value of 5.6 wt.%.

In Fig. 2, curves that are marked with #A–#C are measured in the desorbed state, after the DSC experiments. Desorption at low hydrogen pressures (3 bar H_2, #A) results in an imide IR absorption with two peaks around 3183 and 3164 cm^{-1}, suggesting formation of an imide type phase where –NH is bonded to a mixture of Li and Mg ions, respectively. After heating pristine samples in 60 bar H_2 to 240 °C, i.e. just above the exothermic transition (#B) $LiNH_2$ and $Mg(NH_2)_2$ lines are observed in the IR spectra. These phases are confirmed by XRD data (see Fig. 3 marked with #A and #B). This agrees with reports that $Mg(NH_2)_2$ is also formed during annealing of $2LiNH_2$–MgH_2 in 100 bar H_2 [3]. Raising the temperature to 350 °C (in 60 bar H_2) yields the MgNH phase (#C).

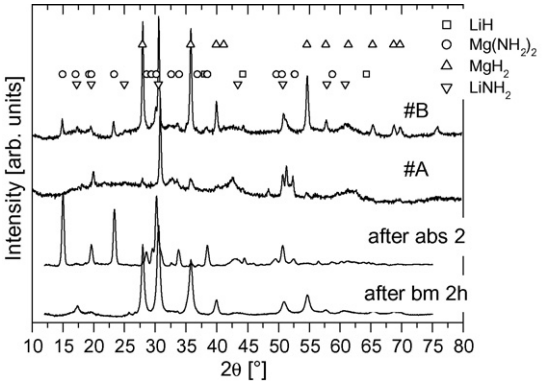

Fig. 3. XRD data at various points of the reaction: (a) after ball milling 2 h, (b) after two re-absorption cycles, (c) after decomposition (until 350 °C) under a static pressure of 3 bar H_2 and (d) after heating under 60 bar H_2 to 240 °C.

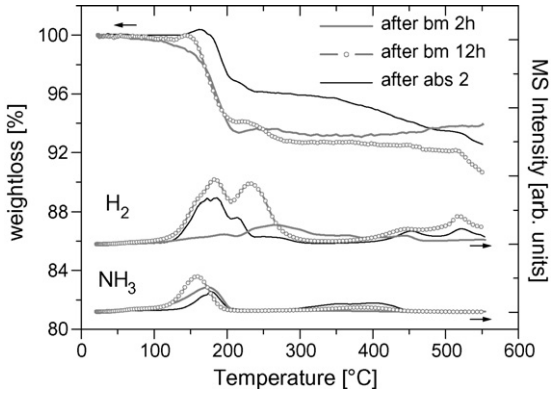

Fig. 4. Weight loss and thermal desorption spectroscopy data for H_2 and NH_3 after 2 h milling, 12 h milling and after two sorption cycles.

The hydrogen decomposition reaction occurs in several steps as can be seen from Fig. 4. Here, the weight loss and the mass spectrometry signal for hydrogen and ammonia are shown as function of temperature. The heating rate for the experiments was 3 K/min, the measurements were performed in high vacuum ($< 4 \times 10^{-6}$ mbar). After ball milling 2 h (open circles) the main hydrogen desorption peaks around 270 °C. However, the weight loss starts much earlier and this transition is accompanied by an intense ammonia signal. Prolonged ball milling for 12 h shifts the hydrogen desorption to lower temperatures although the ammonia evolution persists. The ratio of the released species has shifted in favor of hydrogen. Apparently, the main hydrogen emission consists at least of two distinctive steps. Of these two, only the first involves ammonia. A similar pattern is observed for the reversible reaction after two hydrogenation cycles (open squares): the hydrogen signal exhibits several distinct peaks of which only the first one is accompanied by an ammonia signal. Above 400 °C the imide phase decomposes further and two more H_2 peaks occur.

These finding support an ammonia mediated reaction mechanism as it was also suggested for the $LiNH_2$–LiH system [5]. Presumably, as a first step $Mg(NH_2)_2$ decomposes into MgNH and ammonia which then reacts with the LiH to $LiNH_2$. For the subsequent steps several pathways are possible:

(1) MgNH reacts with the newly formed $LiNH_2$ under the emmision of hydrogen;
(2) MgNH reacts with LiH;
(3) $LiNH_2$ decomposes into Li_2NH which subsequently reacts with MgNH to form a $Li_2Mg(NH)_2$ as was suggested by Leng et al. [6].

In order to evaluate the options listed above, MgNH + $2LiNH_2$ (1) and MgNH + 2LiH (2) mixtures were prepared in a mortar. After mixing, X-ray diffraction patterns show only the starting materials. The powders were subsequently heated to 450 °C and kept for 30 min. Fig. 5 shows the diffraction patterns after the heat treatment. In sample (1), Li_2NH is formed and there is a scarce peak of Mg_3N_2. However it seems that most of the Mg is not contained in an established Mg–N based crystalline phase while two unidentified reflection appear at 17.52° and

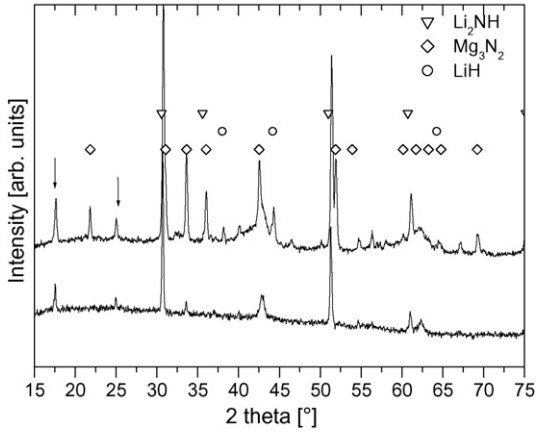

Fig. 5. X-ray diffraction pattern of MgNH+2LiH (upper curve) and MgNH + $2LiNH_2$ (lower curve) after heat treatment at 450 °C in 3 bar H_2.

24.95°. Sample (2) exhibits diffraction peaks of Mg_3N_2 and Li_2NH as can be expected from the decomposition of MgNH into the nitride phase under the emission of ammonia which then reacts with LiH to Li_2NH. Furthermore, unreacted LiH remains in the sample and the peaks at 17.52° and 24.95° are also observed. Remarkably, the unidentified peaks around 17.52° and 24.95° can be indexed in the unit cell of Li_2NH [12] as reflection (1 0 0) and (1 1 0). In pure Li_2NH the structure factor for these reflection vanishes due to the symmetry of the unit cell. However, if some Li is substituted by Mg the symmetry would be lowered and the reflections could be allowed. These experiments confirm that a mixed LiMg-imide phase could be formed.

3.2. The addition of $TiCl_3$

In Fig. 6, pure $2LiNH_2$–MgH_2 mixtures are compared with a sample that contained 2 mol% $TiCl_3$. Fig. 6(a) shows the DSC measurements of pristine samples that were ball milled 2 h with and without added $TiCl_3$. Apparently, the exothermic formation of $Mg(NH_2)_2$ remains unchanged upon the addition of $TiCl_3$ while the endothermic hydrogen release reaction is shifted to lower temperatures. For the data shown

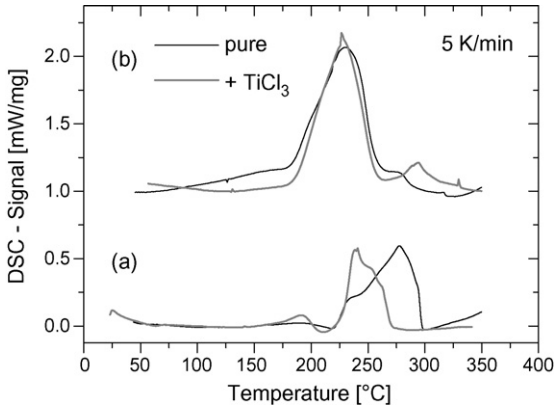

Fig. 6. DSC measurements of $2LiNH_2$–MgH_2 mixtures with added $TiCl_3$. (a) $TiCl_3$ added at initial milling (2 h), (b) $TiCl_3$ added after two hydrogenation cycles. For clarity the curves shown in (b) have been shifted along the vertical axis.

in (b) $TiCl_3$ was added after completion of two desorption/absorption cycles. Both powders were treated in the same way, i.e. after cycling they were again ball milled for 30 min at 400 rpm. If $TiCl_3$ is added to the reversible reaction (reaction 2) there is no benefit from the additive. Although we observe a lower decomposition temperature after adding $TiCl_3$ to the initial mixture, this effect can also be obtained by long ball milling times (compare Fig. 1, 12 h ball milling). For SiO_2 based additives, we obtain similar results. It seems likely that these additives mainly enhance the milling intensity and speed up grinding and homogenization of the $2LiNH_2$–MgH_2 mixture. They do operate on the reversible hydrogen storage reaction.

4. Conclusions

We presented a study on the sorption properties of ball milled $2LiNH_2$–MgH_2 mixtures. During the first desorption cycle or intense ball milling $Mg(NH_2)_2$ is formed which then is part of the reversible reaction. The desorption involves various steps: most likely, initially $Mg(NH_2)_2$ emits ammonia which then reacts with the binary hydride LiH to form $LiNH_2$. In a second step, MgNH and either $LiNH_2$ or LiH react to form a mixed LiMg -imide phase. The addition of $TiCl_3$ enhances the milling intensity and hence lowers the desorption temperature but it does not have a catalytic effect on the reversible reaction.

Acknowledgment

Partial funding by the European Commission DG Research (contract SES6-2006-518271/NESSHY) is gratefully acknowledged by the authors.

References

[1] J.J. Vajo, F. Mertens, J. Phys. Chem. B 109 (2005) 3719.
[2] P. Chen, Z. Xiong, J. Luo, J. Li, K.L. Tan, Nature 420 (2002) 302.
[3] W. Luo, E. Rönnebro, J. Alloys Compd. 404–406 (2005) 392.
[4] W. Luo, S. Sickafoose, J. Alloys Compd. 407 (2006) 274.
[5] T. Ichikawa, H.Y. Leng, S. Isobe, N. Hanada, H. Fujii, J. Power Sources 159 (2006) 126.
[6] H. Leng, T. Ichikawa, H. Fujii, J. Phys. Chem. B 120 (2006) 12964.
[7] O. Kircher, M. Fichtner, J. Appl. Phys. 95 (2004) 7748.
[8] Z. Xiong, J. Hu, G. Wu, P. Chen, W. Luo, K. Gross, J. Wang, J. Alloys Compd. 398 (2005) 235.
[9] H. Leng, T. Ichikawa, S. Hino, N. Hanada, S. Isobe, H. Fujii, J. Power Sources 156 (2006) 166.
[10] G. Linde, R. Juza, Z. Anorg. Allg. Chem. 409 (1974) 199.
[11] Y. Kojima, Y. Kawai, J. Alloys Compd. 395 (2005) 236.
[12] T. Nortake, H. Nozaki, M. Aoki, S. Towata, G. Kitahara, Y. Nakamori, S. Orimo, J. Alloys Compd. 393 (2005) 264.